Multi-turn High Frequency Co-axial Winding Power Transformers

Mark S. Rauls, Donald W. Novotny, Deepakraj M. Divan, Robert R. Bacon, R.W. Gascoigne

Department of Electrical and Computer Engineering
University of Wisconsin-Madison
1415 Johnson Drive
Madison, WI 53706

Abstract - **Previous papers on co-axial winding transformers have focused on designs which use a copper tube to form a single turn outer winding, and litz wire for a multiple turn inner winding. In high power applications the increased resistance of a solid outer winding due to skin effect can be a limiting factor in achieving good performance, especially at frequencies above several hundred kHz. A single turn outer winding leads to large core cross section areas at lower frequencies and the turns ratio is limited to a ratio of 1:n, where n is an integer. This paper demonstrates several methods for achieving multi-turn outer windings to improve design flexibility for the co-axial winding transformer. Experimental measurements on transformers which have multi-turn outer windings are included to confirm analytical results and demonstrate the modified designs.**

Introduction

One of the major concerns in high frequency power conversion is the question of magnetic component design. The use of co-axial transformers for high-frequency, high-power converters was proposed in reference [1]. The co-axial transformer concept has been used with considerable success in various converters including a 50 kHz, 50 kW dual active bridge dc/dc converter and a 600 W, 1 MHz dual resonant dc/dc converter.[2,3] The influence of skin effect on winding resistance and the variation of core loss caused by non-uniform flux density were examined in [4]. These previous papers have focused on designs which have a single turn outer winding constructed from copper tubing as shown in Fig. 1. As can be seen, it is possible to realize integral turns ratios with this topology by using multiple turns on the inner winding. However, the transformer turns ratio is restricted to a ratio of 1:n, where n is an integer. The single turn outer winding can also require large core cross section area at lower frequencies and result in a transformer which is non- optimal in both cost and physical size. At very high frequencies the single turn solid copper tube winding can become a limiting factor in terms of the very small skin depth which limits the current capacity of the winding. Thus while the use of litz wire for multi-turn winding can help control skin effect in the inner winding, the solid copper tube outer winding becomes the limiting element of the design.

There are, therefore, a number of reasons to consider

0-7803-0634-1/92$03.00 ©IEEE

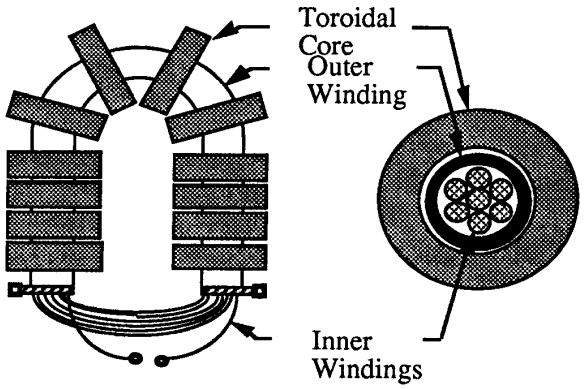

Fig. 1 Co-axial Winding Transformer

methods for attaining multi-turn outer windings while preserving the many advantages of co-axial winding structures. Two basic approaches are considered in this paper; one which employs modifications of the original solid copper tube outer winding structure and a second approach which utilizes litz wire for both the inner and outer windings.

Skin Effect in Co-axial Structures

Since skin effect in the conductors of high frequency transformers is an important limiting factor, it is useful to consider its physical origin to aid in understanding the results which follow. Skin effect is the generic term used to describe the redistribution of current and the associated increase in resistance of conductors as the excitation frequency increases. Although the phenomenon can be physically interpreted in a variety of ways, it is most useful to visualize it as an eddy current effect for the frequency range and type of structures of interest.

Fig. 2 illustrates this concept in a co-axial structure. The inner conductor establishes a magnetic field (B in Fig. 2) which exists in the conducting material of the outer conductor. The current in the outer conductor also affects the B-field and the total field is zero outside the outer conductor. However, since the magnetic field in the outer conductor is time varying it induces a voltage which in turn causes an eddy current in the outer conductor as shown in Fig. 2. The eddy current adds to the conduction current at the inner surface and subtracts at the outer surface creating a non-uniform current distribution by

crowding the current to the inner side of the outer tube, resulting in increased total I^2R loss.

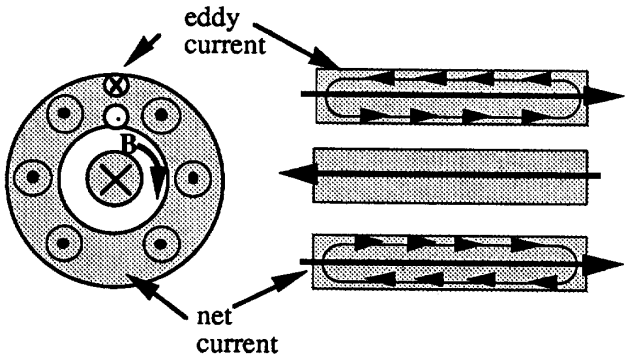

Fig. 2 Qualitative Illustration of Eddy Current in Outer Conductor of co-axial Winding

There would also be an eddy current in the inner conductor (not shown in Fig. 2) which opposes the conductor current in the center and adds at the surface. Note that there would be an eddy current in the outer conductor even if it carried zero net current (no conduction current). In fact, the eddy current would be larger since the net magnetic field is larger without the compensating effect of the return current. Eddy currents caused by currents in adjacent conductors are often called proximity effects while self-induced eddy currents are referred to as skin effect eddy currents. Note that this differentiation becomes complicated when both conductors carry current.

One of the major advantages of co-axial structures is that the magnetic field has circular symmetry which inherently avoids leakage fields which enter the outer conductor in the radial direction. Such fields would clearly have an eddy current path of large area and could result in very high conductor eddy currents. The leakage flux is also entirely outside the magnetic core which avoids local regions of high core flux density.

Litz wire, composed of many fine wires woven in a pattern which transposes the strands in a manner to equalize the induced voltage, is widely used in high power, high frequency transformers. If properly selected and terminated it is capable of controlling skin and proximity effects over a wide range of frequencies. Problems often occur near the terminations because of the necessity to bring all the strands to a common point. It has performed very well as the inner, multi-turn winding of a number of prototype co-axial winding transformers.

Multi-turn Windings using Concentric Tubes

One obvious way to create a multi-turn co-axial winding is to use concentric solid copper tubes connected in series as illustrated in Fig. 3. From the qualitative discussion of the previous section it is expected that the skin effect losses in the inner tube will be substantially higher than in the outer tube because the magnetic field is larger. The larger field is a result of having only one half of the ampere-turns which oppose the center conductor ampere turns in the inner tube and to a much less extent because it is closer to the center conductor. The degree of increase of the winding loss is an important issue and is examined in the following section.

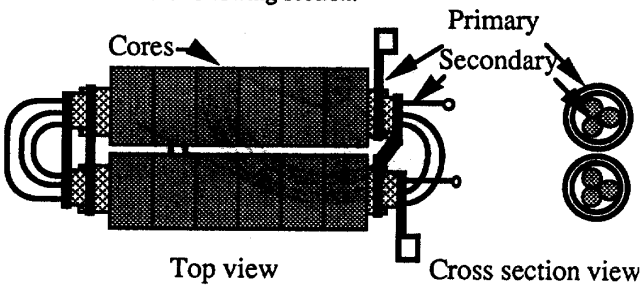

Fig. 3. Transformer with Two Turn Outer Winding Using Concentric Solid Tubes

A. AC Resistance of Series Connected Concentric Tubular Windings

By assuming cylindrical symmetry and sinusoidal time variation, the current density in a solid cylindrical conductor is a function of the radius only and is described by Bessel's differential equation of order zero,

$$\frac{d^2J_z}{dr^2} + \frac{1}{r}\frac{dJ_z}{dr} - j\frac{\omega\mu}{\rho}J_z = 0 \qquad (1)$$

where J_z is the peak phasor representing the current density in the z direction, and r is the radial distance from the axis of symmetry. The general solution of (1) involves a linear combination of the modified Bessel functions I_0 and K_0

$$J_z = CI_0\left[\frac{\sqrt{2}r}{\delta}e^{j\pi/4}\right] + DK_0\left[\frac{\sqrt{2}r}{\delta}e^{j\pi/4}\right] \qquad (2)$$

The arbitrary constants C and D are determined by the magnetic field boundary conditions at the inner and outer radius of the tubular conductor and δ is the skin depth.

Fig. 4 shows the dimensions and the net current at each boundary for the two turn structure of Fig. 3 and for a similar three turn structure. The magnetic flux density at each boundary is a function of the net current enclosed and the radial position

$$B = \frac{\mu_o I_{net}}{2\pi r} \qquad (3)$$

Evaluating Eq (3) at the inner and outer surfaces of each conductor yields the boundary conditions needed to find C and D in Eq (2).

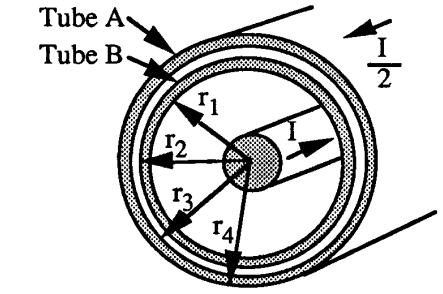

(a)

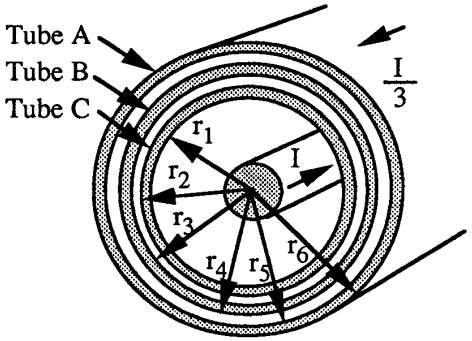

(b)

Fig. 4 Concentric Tubular Winding Dimensions

Finally the ac resistance of the conductor can be expressed in terms of the average power P_{ave} and the rms current

$$R_{ac} = \frac{P_{ave}}{I_{rms}^2} \quad [\Omega/m] \quad (4)$$

where

$$P_{ave} = \frac{1}{2}\int_{r_i}^{r_o}\int_{0}^{2\pi} |J_z(r)|^2 \rho\, r\, d\theta\, dr \quad [W/m] \quad (5)$$

and

$$I_{rms} = \frac{1}{\sqrt{2}}\int_{r_i}^{r_o}\int_{0}^{2\pi} J_z(r)\, r\, d\theta\, dr \quad (6)$$

The resulting integrals are difficult to evaluate in closed form but can be readily found by numerical methods. A closed form expression for P_{ave} has been developed by Perry [5] by using approximations of Bessel functions which provide adequate accuracy when the arguments fall in certain ranges. The result is

$$P_{ave} = \frac{\rho\pi}{8\mu_0^2\delta}[(r_i B_i^2 + r_o B_0^2)F_1(d_n) - (4B_o B_i\sqrt{r_o r_i})F_2(d_n)] \quad [W/m] \quad (7)$$

where the quantities in the expression are defined in Appendix A. This expression is completely general and is within 1% of the exact value when the conductor radii are greater than four skin depths. The expression is also valid for a single turn outer winding.

The ac resistances for the windings of Fig. 4 were computed using numerical methods and Eq. 5 and 6 and the closed form expression of Eq. 7. The results were in agreement. Fig. 5 shows the resistance for each outer tube in Fig. 4a as a function of tube wall thickness. The ac resistance for each tube is normalized to the dc resistance of a tube which has the same inner radius as the tube and has a wall thickness of one δ. Notice that the ac resistance of tube A has the same characteristics as the single tube winding examined in Reference 4 with the minimum ac resistance occurring when the wall thickness is 1.57δ. However, the minimum ac resistance of tube B occurs at a wall thickness of 0.82δ, and its normalized minimum value is 1.63 whereas the minimum for tube A is 0.92. The significant difference in ac resistance between tube A and B is caused by the higher flux density at the location of tube B and the resulting difference in current distribution. In tube A, skin effect causes the current to crowd towards the inner surface. For tube B, the current crowds towards both surfaces of the tube, and the phase of the current at one surface can be partially out of phase with the other surface which results in a very large ac resistance.

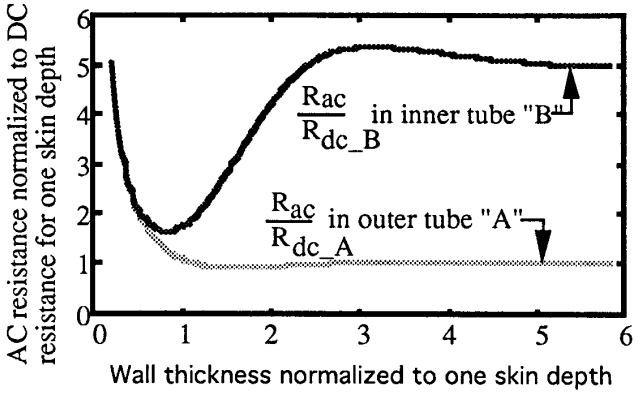

Fig. 5 AC Resistance of the Outer Tubes in Fig. 4a

Fig. 6 shows the resistance for each outer tube in Fig. 4b as a function of tube wall thickness. Again, the ac resistance for each tube is normalized to the dc resistance of a tube which has the same inner radius as the tube and has a wall thickness of one δ. Notice that tube A and tube B have the same ac resistance characteristics for the 3 turn winding as they did in the 2 turn winding. This is because they have the same relative boundary conditions for both winding geometries. Tube C has an even higher resistance than tube B. Its minimum ac resistance occurs at 0.63δ and is 2.1 times the dc resistance for a tube which has the same inner radius and is one δ thick. This is caused by the presence of a magnetic field which is 3 times the relative field which the tube would be subjected to if it were magnetically isolated from the other windings. This suggests that in multi-tube transformers, it is important to regulate copper thickness if high efficiency is to be realized.

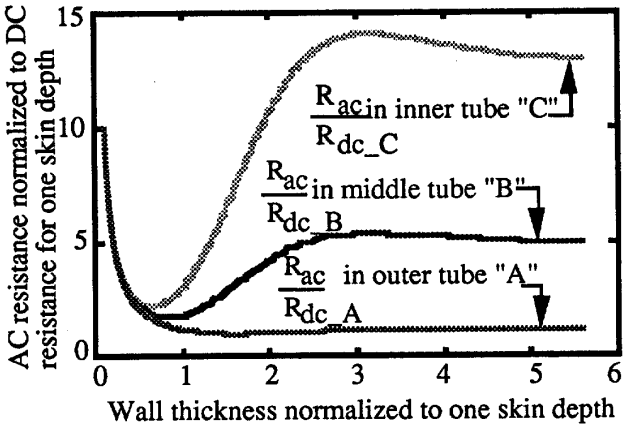

Fig. 6 AC Resistance of the Outer Tubes in Fig. 4b

B. Example of Concentric Multi-turn Resistances

For illustrative purposes suppose that tube thicknesses are chosen to minimize resistance and $r_1 = 10\delta$, $r_3 = 15\delta$, $r_5 = 20\delta$, and let $\delta = 0.3$ mm which corresponds to a frequency near 50 kHz for copper. The resulting per unit length resistances are,

$$\text{Rac\_outer} = 5.11\ \text{m}\Omega/\text{m} \quad (8)$$

$$\text{Rac\_middle} = 12.0\ \text{m}\Omega/\text{m} \quad (9)$$

$$\text{Rac\_inner} = 22.8\ \text{m}\Omega/\text{m} \quad (10)$$

Notice that the innermost tube has a resistance which is nearly 5 times that of the outermost tube. A portion of the added resistance results from the smaller area of the inner tube. These results indicate that special attention must be paid to the tube wall thicknesses and spacing if the ac resistance of concentric, multi-turn, tubular windings is to be minimized. It appears that multi-turn outer windings with more than several turns are impractical due to the large ac resistances of the innermost tubes in the winding. Also, it is more important to make the wall thickness equal to the value which gives minimum resistance due to the very large resistances of tubes which are many skin depths thick. This would need more sophisticated manufacturing techniques at higher frequencies where the skin depth is small.

C. Two Turn Concentric Tube Winding Test

A concentric configuration to measure the resistance of a two turn outer winding was constructed. The test setup consists of two concentric copper tubes with 2 inner litz conductors and is shown in Fig. 7.

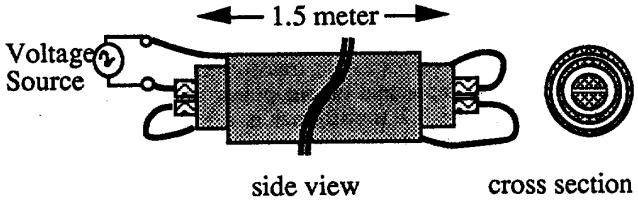

Fig. 7 Laboratory setup for measuring the ac resistance of the 2-turn winding.

The test setup routes current down the outer tube and returns it on one of the litz wires at the center. It is then sent down the inner tube in the same direction as the current in the outer tube, and finally sent back on the remaining litz wire at the center. This simulates a 1:n turn transformer winding where the inner winding carries I and the series connected outer winding carries a current I/n. The theoretical resistance of the setup is plotted with the measured ac resistance results in Fig. 8. The measured results are slightly higher than the theory which is believed to be caused by the solder joints at the end connections.

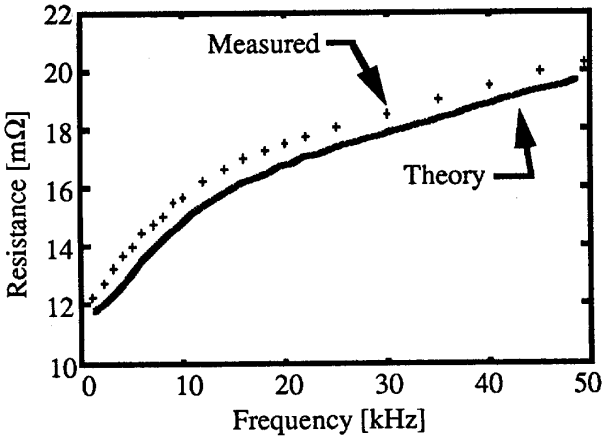

Fig. 8 Measured and theoretical resistance for the 2-turn laboratory setup.

Multi-turn Windings Using Split Tubes

Another way to create multiple turns on the outer winding from a tubular conductor is to split a single tube into sections and connect them in series. Fig. 9 shows the cross section of a 3:2 transformer which has the outer winding split into 2 turns. The series connection forces equal current in the two sections of the outer winding and, if the space separating the sections is small relative to the circumference of the winding cross section, the co-axial symmetry between the outer and inner winding is maintained. To test this idea two transformers were built which were identical except for the outer winding. One transformer had the winding split into 2 turns and the other had only one turn. The transformer designs were not optimized in any way and the purpose of the exercise was to demonstrate the viability of the split tube outer winding as a multiple turn winding. Table 1 shows the efficiency of the two transformers under similar VA stress. The efficiencies for the transformers were determined by measuring the input and output power under full load. The efficiency of the 3:2 transformer is a little less than the 3:1 efficiency because there is less co-axial symmetry in the 3:2 windings due to the way they were constructed and there is an extra solder connection which does not exist in the 3:1 transformer. In a manufacturing environment the symmetry could be made more ideal which would improve the performance.

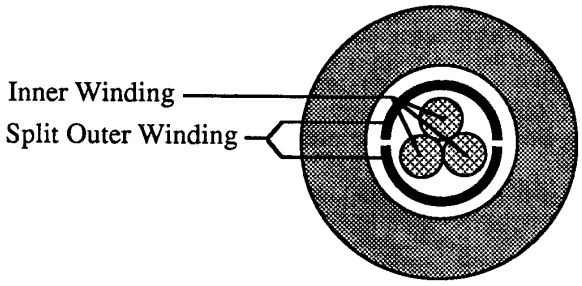

Fig. 9 Cross section for split two turn outer winding, three turn inner winding.

Table 1

Laboratory Data For 3:1 And 3:2 , 250 VA Transformers

Turns Ratio	3:1	3:2
Efficiency	95.3%	94.6%
Primary Voltage	25 V	25 V
Secondary Voltage	8.11 V	15.8 V
Primary Current	10 A	10 A
Secondary Current	28.1 A	14.3 A

Comparison of Concentric and Split Tube Designs

The split tube multi-turn winding preserves the single turn magnetic field distribution and the nearly flat ac resistance characteristic illustrated for tube A in Figs. 6 and 7. However, because the single tube is subdivided into a number of segments, the total winding resistance is increased because each segment has a smaller cross section area and they are connected in series. Assuming the tube is split without losing any material, the resistance of a tube split into n segments will be n^2 times the resistance of the original tube. This will hold for any frequency since the variation with frequency for each segment is exactly like the full tube.

The concentric tube multi-turn winding is quite different in that the magnetic field distribution is different and the resulting ac resistance characteristic is thus very different for each tube. It does, however, allow use of more conductor material and can result in a lower total resistance if each tube is operated close to its optimal wall thickness. Since the optimal thickness is frequency dependent, the concentric tube winding can have a large increase in resistance if the frequency varies. It will also have very different resistance for the fundamental compared to the harmonics in the current waveform.

A simple quantitative comparison between the two schemes can be made under the assumption that the radius of the tube is large compared to the skin depth. For this condition the cross section area of a tube one skin depth thick is well approximated as

$$A \approx 2\pi r\delta \tag{11}$$

and may be taken the same for all tubes in a concentric winding. Defining the resistance of this tube to be R_B, the total resistance of a split tube winding with two turns would be

$$R_s = 4 \times 0.92 \times R_B = 3.68\ R_B \tag{12}$$

if the tube had the optimal thickness of 1.57δ. The corresponding value for a two turn concentric winding is

$$R_c \approx 0.92\ R_B + 1.63\ R_B = 2.55\ R_B \tag{13}$$

where the outer tube has optimal wall thicknesses of 1.57δ and 0.82δ. Note that for approximately 50% more material, the resistance is reduced by about 30%.

If we now consider the corresponding values for the fifth harmonic current, the skin depth will be reduced by $\sqrt{5} = 2.2$. The value of R_B will change, but also the tubes will no longer be of optimal thickness (they will be 2.2 times optimal). Using Fig. 5, the corresponding values of the resistances become

$$R_{s5} \approx 4 \times 1 \times R_{B5} = 4\ R_{B5} \tag{14}$$

and

$$R_{c5} \approx 1 \times R_{B5} + 3.8\ R_{B5} = 4.8\ R_{B5} \tag{15}$$

Table 2

Comparison of Concentric and Split Tube Designs

Turns	Thickness of Innermost Tube	Split Tube Resistance	Concentric Tube Resistance	% Res	% Added material
1	optimal	$0.92R_B$	$0.92R_B$	100	0
1	$>3\delta$	R_B	R_B	100	0
2	optimal	$3.68R_B$	$2.55R_B$	69	52
2	$>3\delta$	$4R_B$	$6R_B$	150	52
3	optimal	$8.28R_B$	$4.65R_B$	56	92
3	$>3\delta$	$9R_B$	$19R_B$	210	92

Optimal Thicknesses (1) 1.57δ (2) 0.82δ (3) 0.63δ

R_B= DC resistance of tube of one δ thickness

which clearly shows that the concentric winding rapidly becomes less effective than the split tube winding when the wall thicknesses are not optimal. Examination of Fig. 5 reveals that when the wall thickness exceeds 3 δ the inner tube resistance approaches five times that of the outer tube yielding a total winding resistance of $6R_B$. Thus for the higher harmonics, the effective resistance of the concentric winding is increased by 50% compared to a split tube winding. The winding losses are also very non-uniformly distributed with the inner winding having five times the loss of the outer winding.

Table 2 summarizes the comparison of the two multi-turn tube type windings for two and three turn windings. When the concentric winding is designed with optimal wall thickness it offers significantly less resistance than a split tube winding; 30% less for two turns and 44% less for three. However, when designed or operated with non-optimal wall thickness the concentric winding will generally have higher resistance, of the order of 50% more for two turns and over 100% more for three turns. The harmonic winding loss will therefore be higher in concentric windings and the distribution of the losses is very non-uniform. However, when harmonic content is small, as for example with triangle wave currents, the concentric winding with optimal wall thickness provides a viable means of reducing winding loss in multi-turn co-axial winding transformers.

Litz Wire Outer Windings

The split tube outer winding of Fig. 9 can clearly be extended to three turns by dividing each tube into three segments. The end connections become more complicated but the principle is valid. The splitting can be carried to n segments in which case the end connections are clearly very complex. However, the division into a large number of segments suggests using wires for the segments which leads to the all Litz wire configuration shown in Fig. 10a. Here the outer winding consists of 14 strands of Litz wire which could form 14 turns or be connected in various series/parallel configurations to give a variety of turns radius. Fig. 10b illustrates another possible all Litz wire configuration in which the outer winding is a hollow cylindrical Litz cable.

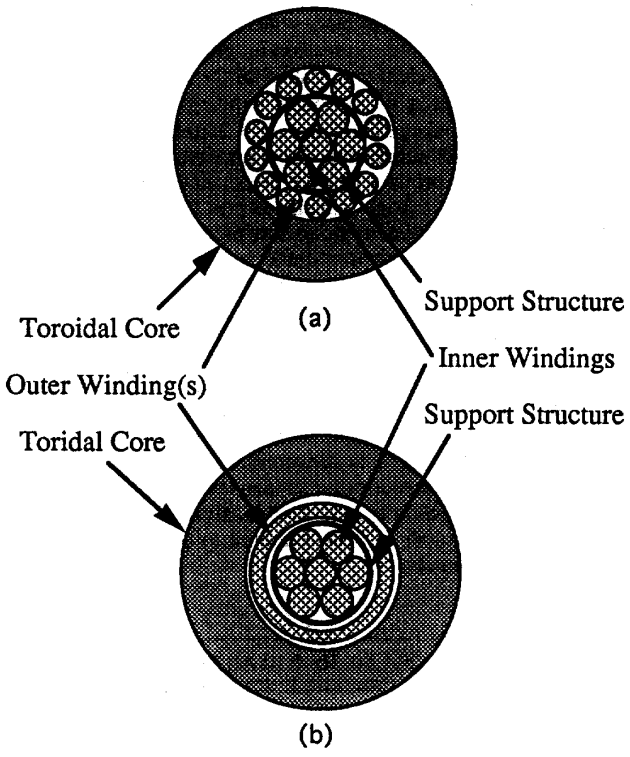

Fig. 10 Litz wire inner and outer windings

Both of these configurations preserve the essential features of co-axial windings although the all Litz wire version in Fig. 10a is only approximately co-axial. This version is, however,

very flexible in terms of obtaining different numbers of turns and a prototype was built and tested using open circuit and short circuit test described in [4]. The experimental unit is shown in Fig. 11 and its data is given in Table 3. The transformer was constructed using a 4 turn inner winding (primary) using 10 gauge litz wire and a 10 turn outer winding (secondary) using 14 gauge litz wire. An end view of the litz winding structure is shown in Fig. 12. PC40 toroids were used as the magnetic medium.

Of major concern when using multiple outer turns is the effect on the leakage inductance. If one were to assume co-axial geometry a leakage prediction can be made as in [1]. The leakage inductance was shown to be

$$L_{leak\_in} = \frac{N_w^2 \mu_0}{8\pi}\left(1 + 4\ln\left(\frac{r_t}{r_{in}}\right)\right) l_{turn} \qquad (16)$$

where N_w is the number of inner winding turns and l_{turn} is the length of one turn. The expression is only approximate here since r_{in} is the equivalent outer radius of the inner winding and r_t is the mean radius of the outer winding. For the given transformer this leakage inductance is 1.05μH. An estimation of the external lead inductance was computed to be .19μH and thus the predicted primary leakage inductance is 1.24μH. The measured primary leakage inductance was found to be 1.4μH which is in close agreement to the predicted value. The winding loss was also measured and was approximately 26% larger then expected, however the error involved in measuring resistance can become significant when the impedance is almost entirely reactive.

This would seem to indicate that the 10 turn outer winding geometry did not significantly increase the leakage inductance compared to that of an ideal cylindrical outer winding and can actually perform better then concentric and split tube designs where end turn connections can cause additional leakage inductance and winding losses. More analysis must be done to determine the number of turns required in order to maintain near co-axial symmetry.

Table 3

Data for 250V, 20A 50kHz 4:10 All Litz Transformer

	Theory	Measured
Secondary Voltage	625V	625V
Secondary Current	8A	8A
Magnetizing Inductance (prim)	1.5-2mH	1.8mH
Leakage Inductance (prim)	1.24μH	1.4μH
Core Loss	20.8W	24.3W
Winding Loss	7.2W	9.1W
Efficiency	99.4%	99.3%

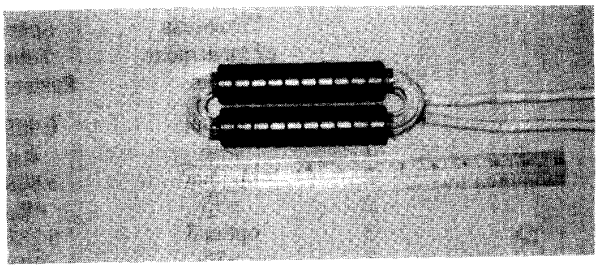

Fig. 11 Photograph of fabricated 5 kVA transformer

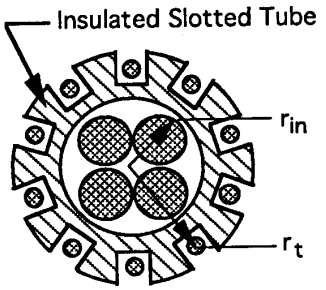

Fig.12 Fabricated litz wire end windings.

Summary

Three methods of attaining multi-turn outer windings in co-axial winding power transformers were proposed and evaluated. Two of the methods utilize solid tube windings; the first employs concentric, series connected tubes and the second uses a single tube split into uniformly spaced arc segments. The concentric tube winding allows use of additional winding material and if the tube thicknesses are chosen close to the optimal values results in the lowest ac resistance increases and ultimately exceeds that of the split tube winding. Most of the winding loss occurs in the inner tube where the magnetic field is highest.

The split tube winding with n turns results in an ac resistance which is n^2 times the resistance of the original unsplit tube. Unlike the concentric tube winding, the frequency dependence of the resistance is identical to the single tube case which can be advantageous when the current has a large harmonic content.

The third technique utilizes litz wire for the outer as well as the inner winding. By employing a number of wires arranged in a cylindrical pattern, a reasonable approximation to a co-axial outer winding can be produced. A prototype transformer having a 10 turn outer winding was constructed and tested.

REFERENCES

[1] M.H. Kheraluwala, D.W. Novotny, D.M. Divan, "Design Considerations for High Frequency Transformers", IEEE-PESC90 Record, pp. 734-742.

[2] M.H. Kheraluwala, R.W. Gascoigne, D.M. Divan, E. Bauman, "Performance Characterization of a High Power Dual Active Bridge DC/DC Converter", IEEE-IAS90 Record, pp. 1267-1273.

[3] H.L.N. Wiegman, D.M. Divan, D.W. Novotny, R. Mohan, "A ZVS Dual Resonant Converter For Battery Charging Applications", IEEE-PESC91 Record, pp. 202-208.

[4] M.S. Rauls, D.W. Novotny, D.M. Divan, "Design Considerations For High Frequency Co-axial Winding Power Transformers", IEEE-IAS91 Record, pp. 946-952.

[5] M.P. Perry, Low Frequency Electromagnetic Design, Chapter 3, Marcel Dekker, 1985.

[6] M.S. Rauls, Analysis And Design Of High Frequency Co-axial Winding Power Transformers, University of Wisconsin - Madison, 1992.

Appendix A

The quantities in Eq. 7 are

r_i = n'th tube inner radius

r_o = n'th tube outer radius

$$d_n = \frac{(r_o - r_i)}{\delta}$$

$$B_i = \frac{\mu_0 Inet\_i}{2\pi r_i}$$

$$B_o = \frac{\mu_0 Inet\_o}{2\pi r_o}$$

Inet_i = net rms current enclosed by the circle at r_i

Inet_o = net rms current enclosed by the circle at r_o

$$F_1(x) = \frac{\sinh(2x) + \sin(2x)}{\cosh(2x) - \cos(2x)}$$

$$F_2(x) = \frac{\sinh(x)\cos(x) + \cosh(x)\sin(x)}{\cosh(2x) - \cos(2x)}$$